Electronic Supplementary Material (ESI) for ChemComm.

HPO_3^{2-} as Building Unit for Sodium-Ion Battery Cathode: 3.1 V Operation of $Na_{2-x}Fe(HPO_3)_2$ ($0 < x < 1$)

Zihan Ma[1†], Laura Lander[1†], Shin-ichi Nishimura[1,2], Masashi Okubo[1,2], Atsuo Yamada[1,2,*]

[1]*The University of Tokyo, Hongo 7-3-1, Bunkyo-ku, Tokyo 113-8656, Japan.*
[2]*ESICB, Kyoto University, Nishikyo-ku, Kyoto 615-8245, Japan.*

**e-mail address of corresponding author: yamada@chemsys.t.u-tokyo.ac.jp*
[†]These authors contributed equally

Supporting Information

Experimental Section

Synthesis: The hydrothermal synthesis method and structure of $Na_2Fe(HPO_3)_2$ have been previously reported by W. Liu *et al.*[20] However, we found that preparing $Na_2Fe(HPO_3)_2$ following the synthesis protocol for its Ni-based counterpart $Na_2Ni(HPO_3)_2$[21] using a solvothermal approach, we obtain a higher reproducibility of the reaction outcome. 2 mmol of $FeCl_2{\cdot}4H_2O$ (Wako, 99%), 32 mmol of H_3PO_3 (Wako, 97%) and 30 mmol of NaOH (Kanto, 97%) were added into a mixed solution of 20 ml methanol (Wako) and 5 ml of distilled water. The 2mmol of L-phenylalanine ($C_6H_5CH_2CH(NH_2)CO_2H$) which was also added by W. Maalej *et al.* seemed to be unnecessary in our synthesis. The suspension was stirred at room temperature until it was homogeneous and then transferred into a 23 mL Teflon™-lined Parr autoclave. Note that all the operations were conducted in an Ar filled glovebox to avoid oxidization of Fe^{2+} to Fe^{3+}, which would lead to the formation of impurities in the final product. The under Ar sealed autoclave was heated at 150 °C for 48 hours. Recovered by filtration, the light grey-colored compound was washed with water and ethanol and then dried at 80 °C in air. In a similar way, the series of $Na_2M(HPO_3)_2$ (M=Mg, Mn, Fe, Co, Ni) could be synthesized using the respective precursors $MCl_2{\cdot}nH_2O$. Unfortunately, the compounds with Mg, Mn, Co and Ni seemed to be electrochemically inactive.

The *in situ* carbon coating was conducted by adding 0.5 mmol sucrose to the precursor solution and stirred until homogeneous. After the thermal treatment (same conditions as described above), the formed powder was recovered and washed with water and ethanol and dried at 80 °C in air.

The chemical extraction of Na^+ from $Na_2Fe(HPO_3)_2$ was conducted by stirring 1mmol $Na_2Fe(HPO_3)_2$ and 1mmol NO_2BF_4 in acetonitrile at room temperature overnight. The compound after chemical extraction was washed with acetonitrile and dried at 80 °C in air.

Characterization: X-ray powder diffraction patterns were acquired in the 2θ range of 10–80° using a Bruker AXS D8 ADVANCE powder diffractometer equipped with a Co $K\alpha$ radiation source operating at 35 kV and 40 mA. High-resolution powder X-ray diffraction pattern was measured at a synchrotron source beamline, BL-4B$_2$ of Photon Factory, Tsukuba, Japan. The Rietveld refinements were conducted with a computer program TOPAS-Academic V6.

^{57}Fe Mössbauer spectra were collected at room temperature with a transmission optics spectrometer (Toplogic System, Inc.). A ^{57}Co dispersed Rh matrix was used as the radiation source and the proportional counter was used for detection of the transmitted γ-ray. α-Fe was used as a standard to calibrate velocity and isomer shift at room temperature. The model fitting was performed with MossWinn 3.0 software.

Particle morphology of powder samples was analyzed with a Hitachi S-4800 field-emission scanning electron microscope operating at 5 kV.

Electrochemistry: The working electrode for electrochemical characterization was formulated by mixing 80 wt% $Na_2Fe(HPO_3)_2$ active material, 15 wt% Ketjen-black (ECP-600JD, Lion Corp.) and 5wt% polytetrafluoroethylene (PTFE) binder. Prompt amounts of N-methyl-2-pyrrolidone (NMP) (Kanto, 99%) were added for better extension of the binder. The loading level of the electrodes for electrochemical tests was controlled to around 5.5 mg cm^{-2}, while for *ex situ* XRD and *ex situ* Mössbauer the loading level was adjusted to around 10 mg cm^{-2}. Electrochemical tests were carried out using 2032-type coin cells. Cells were assembled in an Ar-filled glovebox, using sodium as the anode, two glass fiber filter (GB-100R, ADVANTEC) separators, and 1 M $NaPF_6$ in ethylenecarbonate-dimethyl carbonate (EC/DMC, volume ratio 1:1) liquid electrolyte.

Galvanostatic charge/discharge cycling was conducted with a battery charge-discharge system (TOSCAT 3100, Toyo System Co., Ltd.) in the voltage ranges 1.5–4.5 V *vs.* Na/Na$^+$ at different rates from C/20 to C/2 at 25 °C.

***Ex situ*/*in situ* measurements:** *Ex situ* studies (XRD and Mössbauer) were conducted by retrieving electrodes from the cycled half cells. The cells after running to desired states were disassembled in an Ar-filled glovebox. Positive electrodes were carefully recovered, thoroughly washed with DMC and dried. The electrodes were well-sealed in argon during all measurements.

In situ XRD was conducted using a homemade cell with a Be window on the cathode side. The cell was cycled with a battery charge-discharge system (HJ1020mSD8, Hokuto Denko Corp.) in the voltage range of 1.5–4.5 V at C/20 current rate (at 25 °C) while recording the XRD patterns with a Bruker AXS D8 ADVANCE diffractometer.

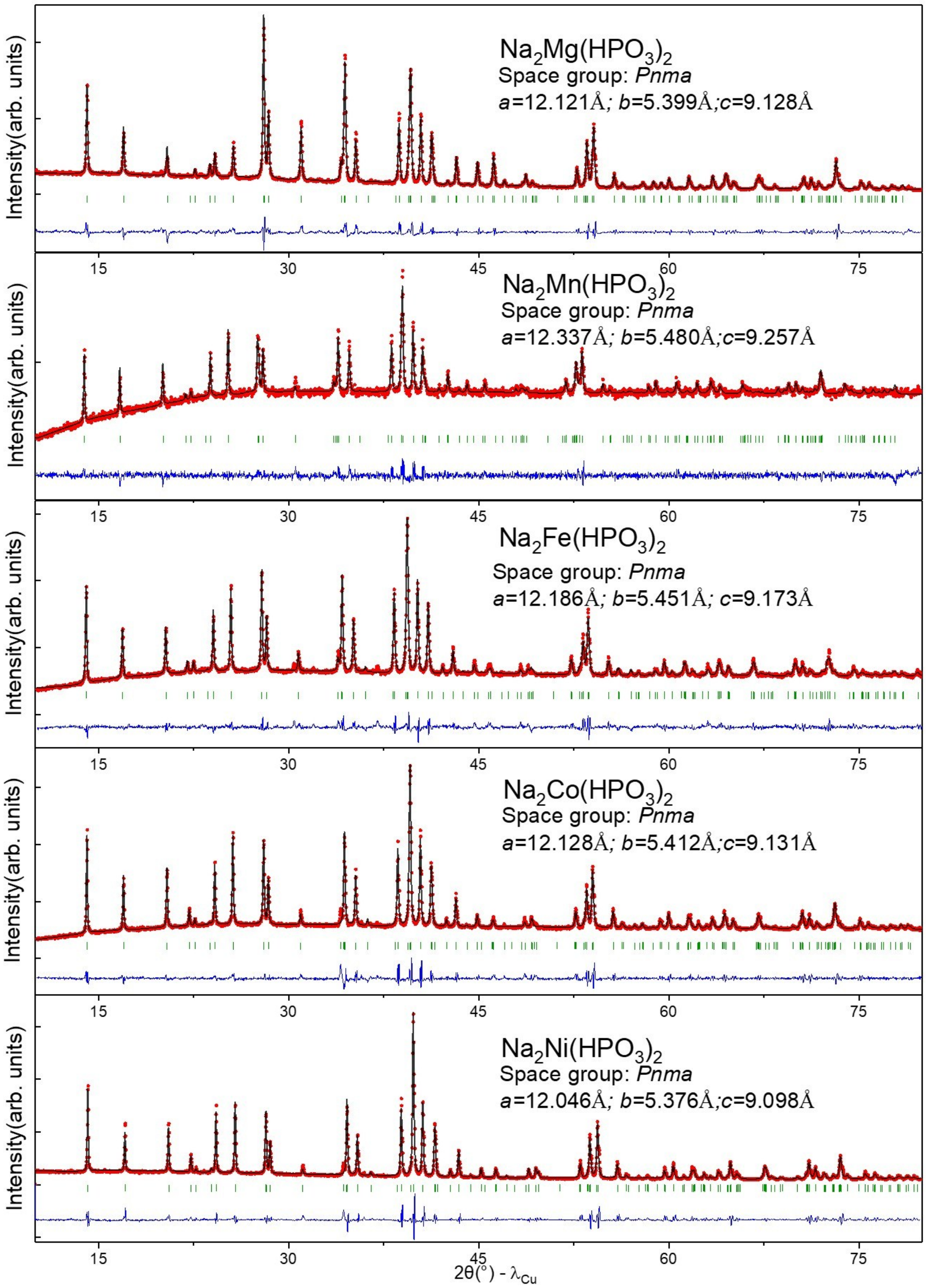

Figure S1. Power XRD pattern and pattern matching of (a) $Na_2Mg(HPO_3)_2$, (b) $Na_2Mn(HPO_3)_2$, (c) $Na_2Fe(HPO_3)_2$, (d) $Na_2Co(HPO_3)_2$, (e) $Na_2Ni(HPO_3)_2$. The red dots stand for the observed, black line for the calculated, blue line stands for difference between the observed and the calculated, green bars stand for bragg positions.

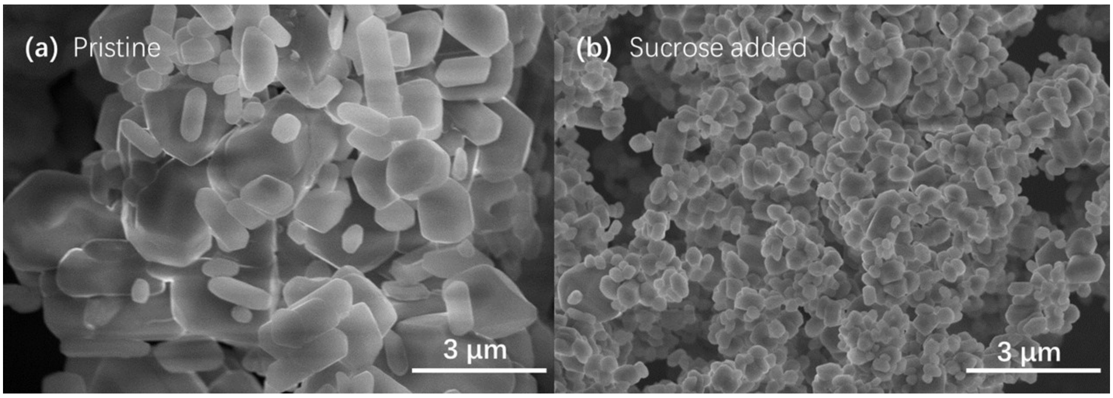

Figure S2. SEM images of (a) products without sucrose and (b) products with sucrose.

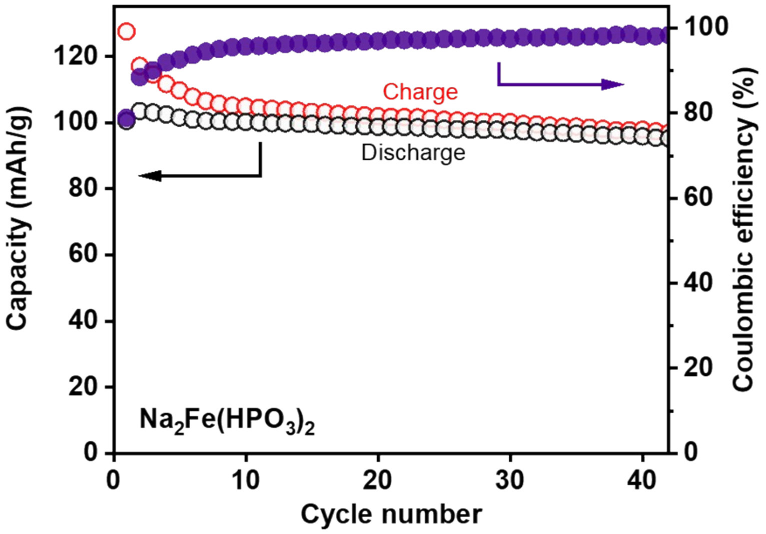

Figure S3. Charge-discharge capacity and coulombic efficiency of $Na_2Fe(HPO_3)_2$ at C/20 rate.

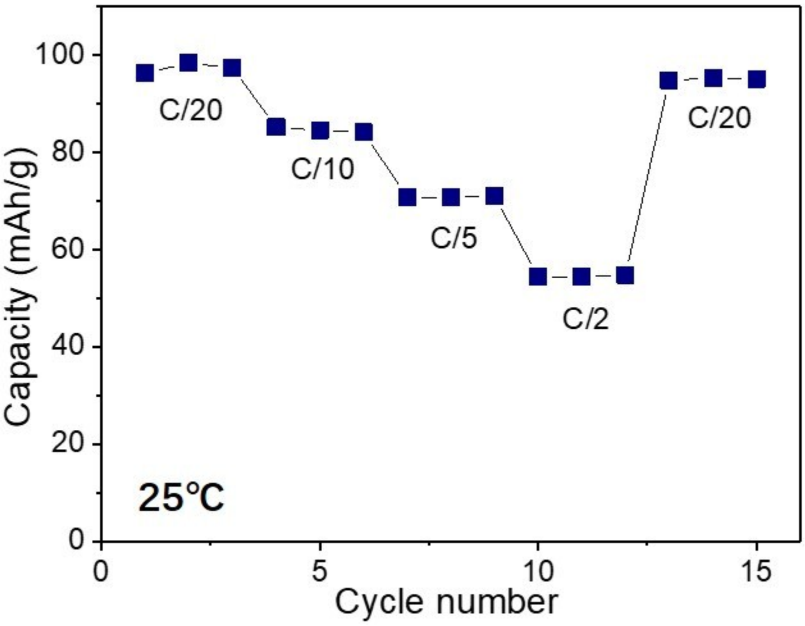

Figure S4. Rate capability test: discharge capacity of $Na_2Fe(HPO_3)_2$ at C/20, C/10, C/5 and C/2 rate.

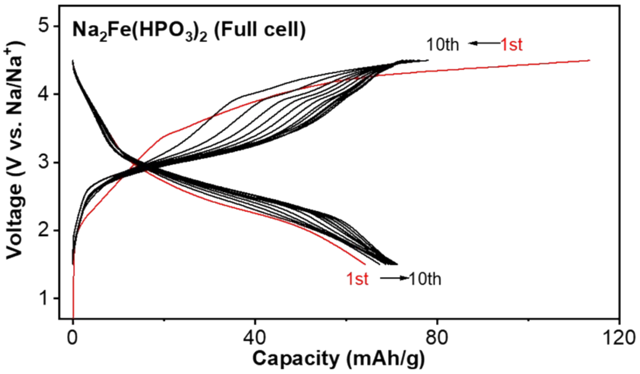

Figure S5. Charge-discharge curves of $Na_2Fe(HPO_3)_2$ – hard carbon full cell between 1.5 and 4.5 V *vs*. Na/Na$^+$ at C/10 rate.

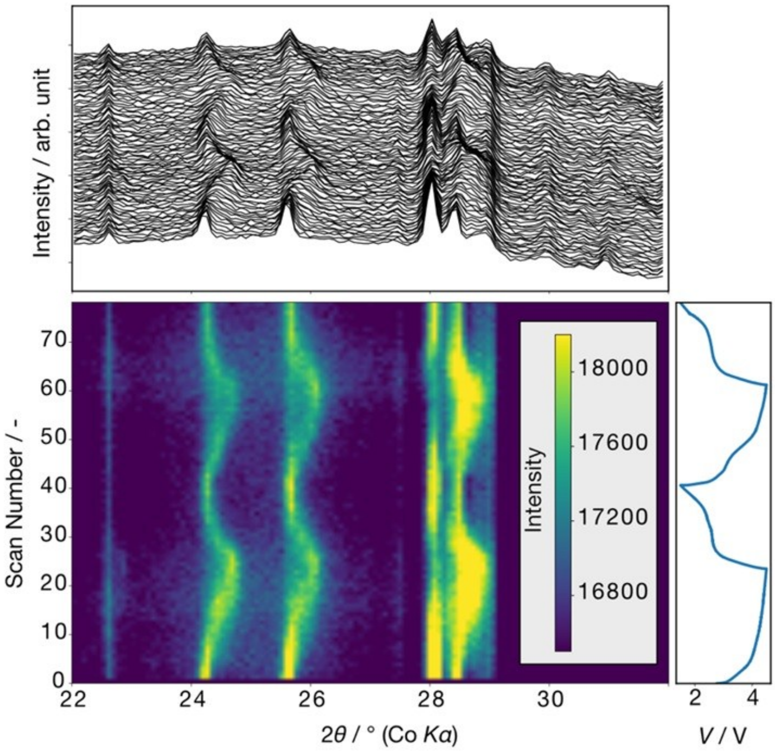

Figure S6. *In situ* XRD of $Na_2Fe(HPO_3)_2$ at C/20 rate.

(a)

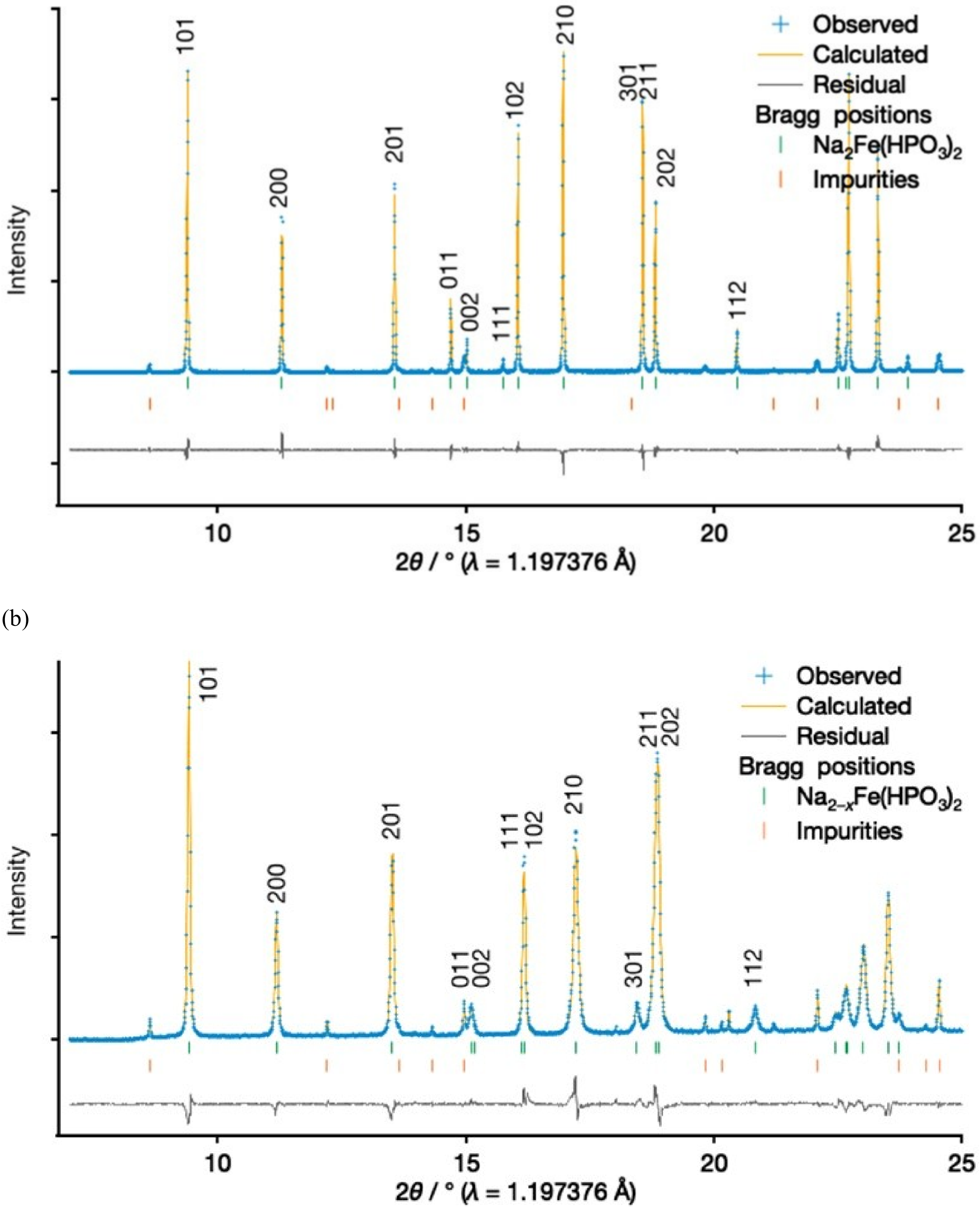

(b)

Figure S7. X-ray diffraction patterns and Rietveld refinement of (a) pristine and (b) chemically oxidized $Na_xFe(HPO_3)_2$.

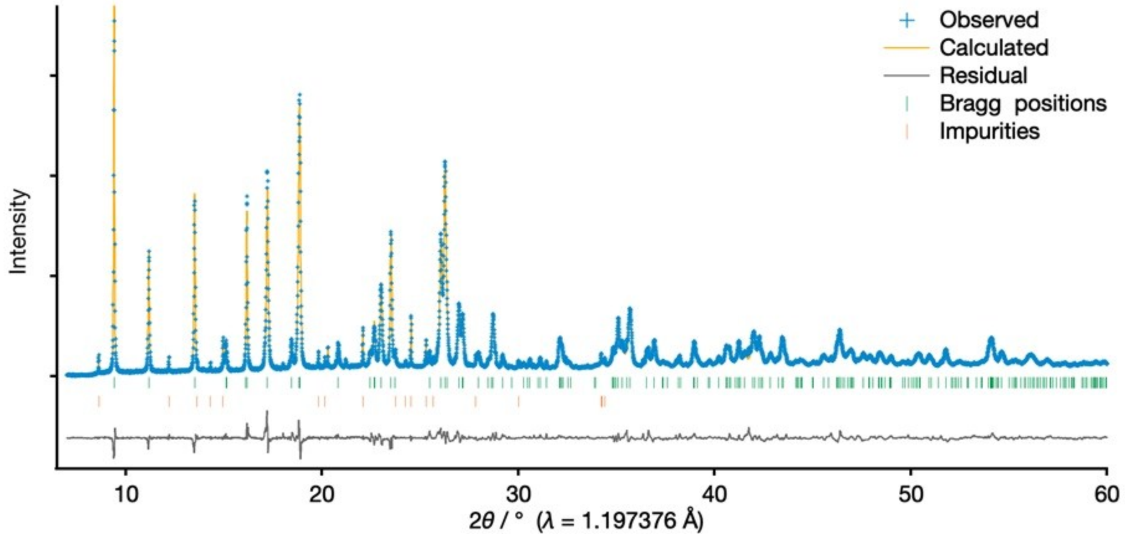

Figure S8. Rietveld refinement of chemically oxidized $Na_xFe(HPO_3)_2$. The *R*-indices were converged R_{wp} = 7.63%, R_p = 6.04%, R_{Bragg} = 2.89%, and $GoF = R_{wp}/R_e = 2.61$.

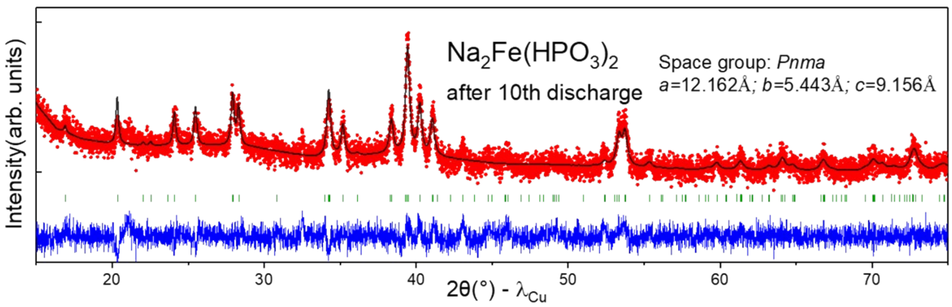

Figure S9. XRD profile and pattern matching of 10−time cycled $Na_2Fe(HPO_3)_2$ electrode.

Table S1 Wyckoff notations, fractional coordinates, occupancy factors, and atomic displacement parameters of the each atomic sites for the as prepared $Na_2Fe(HPO_3)_2$*.

Sites	Wyckoff	x	y	z	g	B / Å$_2$
Fe	4*c*	0.15966(3)	1/4	0.63647(4)	1	1.004(8)
P1	4*c*	0.01547(5)	–1/4	0.62828(7)	1	0.984(13)
O11	4*c*	0.10529(13)	1/4	0.41767(18)	1	1.93(4)
O12	8*d*	0.04790(10)	–0.0207(2)	0.71290(12)	1	1.80(4)
P2	4*c*	0.18462(5)	1/4	0.00284(7)	1	1.117(13)
O21	4*c*	0.23124(13)	1/4	0.84771(18)	1	1.80(4)
O22	8*d*	0.28602(10)	–0.0171(2)	0.58486(12)	1	1.71(3)
Na1	4*c*	0.09574(9)	3/4	0.22603(11)	1	1.78(2)
Na2	4*c*	0.27994(8)	1/4	0.32671(11)	1	1.96(2)

*The hydrogen atoms were omitted through the refinement.

Table S2. ^{57}Fe Mössbauer parameters (isomeric shift (IS), quadrupole splitting (QS) and line width (LW)).

		Percentage	**IS (mm s^{-1})**	**QS (mm s^{-1})**	**LW (mm s^{-1})**
pristine (Before cycle)	Fe^{2+}	94.2%	1.24(3)	1.11(2)	0.35(5)
	Fe^{3+}	5.8%	0.37(8)	0.24(5)	0.46(9)
After 1st charge	Fe^{3+}	100%	0.33(1)	0.34(9)	0.37(4)
After 1st discharge	Fe^{2+}	75.8%	1.24(5)	1.11(4)	0.29(3)
	Fe^{3+}	24.2%	0.45(2)	0.39(2)	0.39(9)

Table *S*3 Symmetry and crystal lattice information

	As prepared	Oxidized
Crystal system	orthorhombic	orthorhombic
Space group	*Pnma*	*Pnma*
a / Å	12.186116(19)	12.3044(3)
b / Å	5.449625(7)	5.26941(13)
c / Å	9.170437(13)	9.07982(19)
V / Å^3	609.0066(15)	588.71(2)
Z	4	4

Table S4. Wyckoff notations, fractional coordinates, occupancy factors, and atomic displacement parameters of the each atomic sites for the chemically oxidized $Na_{2-x}Fe(HPO_3)_2$[*].

Sites	Wyckoff	x	y	z	g	B / Å$_2$
Fe	4*c*	0.16555(15)	1/4	0.61903(17)	1	1.91(5)
P1	4*c*	0.0111(3)[§]	–1/4	0.6470(3)[§]	1	2.60(8)[†]
O11	4*c*	–0.0999(6)[§]	–1/4	0.5791(7)[§]	1	3.17(7)[‡]
O12	8*d*	0.0588(4)[§]	–0.0119(8)[§]	0.7008(5)[§]	1	3.17(7)[‡]
P2	4*c*	0.1914(3)[§]	1/4	–0.0199(4)[§]	1	2.60(8)[†]
O21	4*c*	0.2338(5)[§]	1/4	–0.1764(8)[§]	1	3.17(7)[‡]
O22	8*d*	0.2272(4)[§]	0.0072(10)[§]	0.0593(6)[§]	1	3.17(7)[‡]
Na1	4*c*	0.0906(5)	3/4	0.2283(7)	0.585(6)	2
Na2	4*c*	0.2698(6)	1/4	0.3086(9)	0.489(5)	2

* The hydrogen atoms were omitted through the refinement.

† B for P were constrained to be equal.

‡ B for O were constrained to be equal.

§ P—O bond length was restrained to be 1.52±0.01 Å.